Activity report of the Italian CRG beamline at the European Synchrotron Radiation Facility (ESRF)

N. 4 - December 2016

Grenoble, December 2016

71 Avenue des Martyrs, Grenoble, France

Responsabile editoriale: Francesco d'Acapito
(*dacapito@iom.cnr.it*)

Editing: Roberta De Donatis
(*roberta.dedonatis@cnr.it*)

LISA

Annual Report 2016

Istituto Officina dei Materiali

Abstract

This document resumes the activity of the Italian CRG beamline at ESRF (LISA project) during year 2016. Statistic data on the beamline use are presented as well as the latest major instrumental advancements, highlight experiments and publications.

Keywords

Italian beamline at ESRF, BM08

LISA project

X-ray Absorption Spectroscopy

Index

Foreword

The realization of the LISA project is now under full swing. Right after the summer shutdown the electrical and ethernet distribution networks have been renewed due to the obsolescence of the previous material and it is now fully operative. This upgrade has partially impacted the user activity with a shutdown in the period August-September. The procurement of the principal components (monochromator, mirrors, cryocirculator) has been completed and the installation of the new devices will take place in the first months of year 2017. This will lead to a temporary closure of the beamline in two phases: the first during run 1-17 (Jan-Mar) for the installation of the monochromator and the second in run 4-17 (Aug-Oct) for the installation of the new mirrors and experimental bench. Users will be informed in due time on the available “user mode” periods of activity.

The final Conceptual Design Report (CDR) of the beamline has been completed with the choice of a Super Bend source and it has submitted to the ESRF Scientific Advisory Committee (SAC) in its spring meeting. The SAC has analyzed the proposal and has endorsed the continuation of the beamline activity. The super bending magnet (SBM) source will ensure a beam free from spurious contributions from other sources in the machine and will allow to fully benefit from the increased brightness of the Extremely Brilliant Source (EBS) ring.

At present a complete staff is working on the beamline for the standard and refurbishment operations: F. d’Acapito, A. Puri and G. Lepore (CNR-IOM-OGG Grenoble) constitute the local scientific staff and they are supported by A. de Luisa (CNR-IOM-Trieste) for the mechanical design and drawings and E. Dettona (ESRF, Grenoble) for the interface and coordination with the ESRF technical services. From the point of view of the scientific activity this year has been particularly productive; during this year 32 experimental sessions have been carried out for a total amount of 432 shifts. The publications appeared in year 2016 are 28 out of which 7 on high impact (IF>7) journals. During year 2016 LISA has hosted students for stages, Giulia Fantappiè and Andrea Giaccherini from the Florence University and Chiara Petroselli form the Perugia University. A roundtable with the Italian community was held during the Italian Synchrotron Radiation Society (SILS) meeting (Bari, Sept 2016) for the definition of the possible activities and future projects with the Italian user community.

In the course of year 2016 the choice of the LISA source on EBS has been finalized. ESRF offered 4 kind of sources on the new EBS ring to the Collaborating Research Groups (CRG):

- The new bending magnets
- 3 pole wiggler
- 2 pole wiggler
- Super Bending Magnet (SBM)

Considered the need to have a beam at high energy and free from residual contributions from the other magnetic elements of the cell, the SBM source has been retained. It will be placed between the DQ2C and DQ1D magnets (Fig.1 left) and it will have a magnetic field of 0.85 T so maintaining the same critical energy as nowadays. The electron beam under the SBM will be highly brilliant with a size of 23(hor) * 3.6 (vert) μm RMS and a divergence of 24(hor) * 3(vert) μrad RMS. Its emission is well separated from the other magnets (Fig.1, right) so constituting a clean source well adapted to microfocus applications.

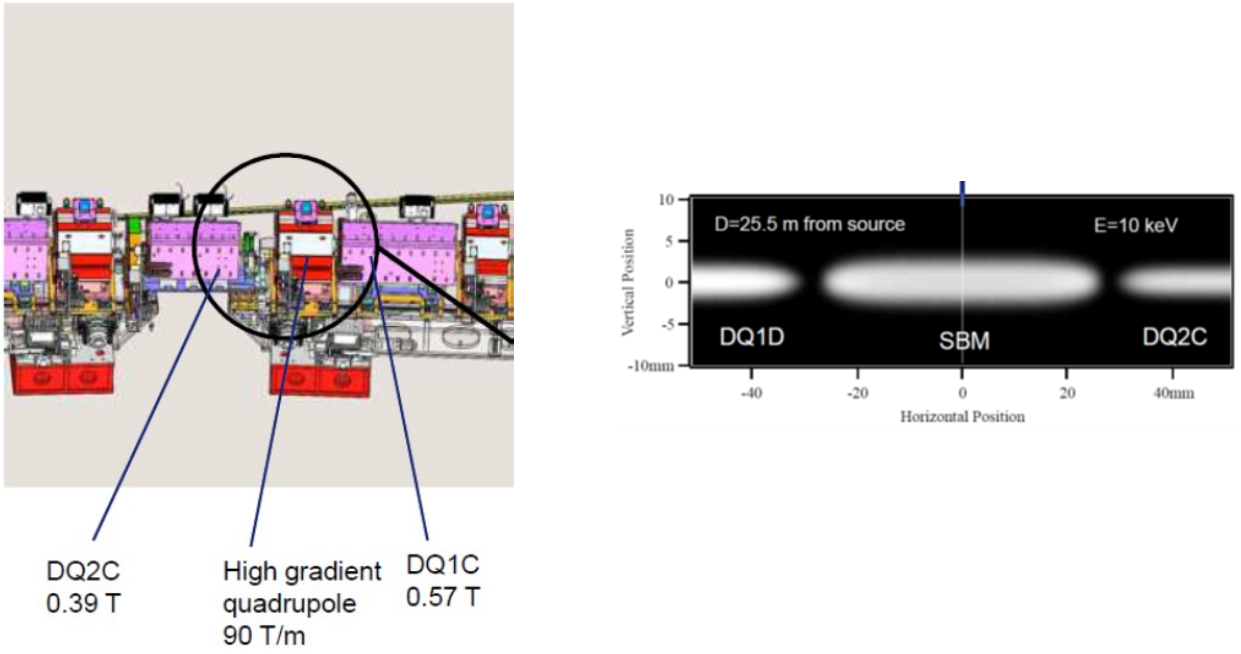

Fig.1. Left: the black circle marks the location of the new source for LISA in the EBS ring. It will be placed in the space between the DQ2C dipole and the High gradient quadrupole. Right: Simulated emission of the SBM at 25.5 m from the source showing the clear separation of its emission respect to the preceding DQ2C and following DQ1D dipoles. Credits: J. Chavanne, ESRF

The layout of the new beamline has been finalized and it is shown in Fig.2:

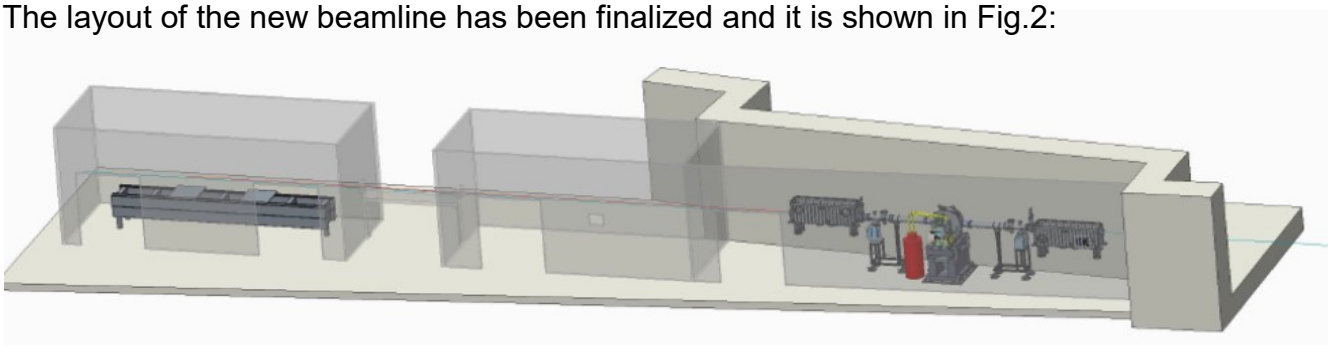

Fig.2 Layout of the LISA beamline as it will appear after the completion of the refurbishment (foreseen Oct 2017).

On the right side the optic hutch is shown with the new mono (central vacuum chamber) on its granite support and the cryocirculator (red). The new mirrors will be installed in the pre-existing vessels (before and after the mono). The new XAS station will be installed in the EH2 (left side of Fig.1) and will consist in a long bench with space to allocate the old sample chambers and users' instrumentation. Wide space will be available for sample environment mounting in air or in vacuum at choice. The instrumentation in the first experimental hutch will remain available for experiments not needing beam focusing. A detailed description of the project can be found in the LISA web page.

The electrical and Ethernet distribution networks have been completely renewed. A new electrical cupboard has been installed and new sockets are now present in the hutches. Those sockets are now standard 'French' models that are no longer compatible with previously used 'Italian' plugs. If you are planning to bring instruments with you for your experiment at LISA please ensure that your plugs are compatible with the new sockets.

Tuning the energetics and tailoring the optical properties of silver clusters confined in zeolites

Oliver Fenwick[1], Eduardo Coutiño-Gonzalez[2], Didier Grandjean[3], Wouter Baekelant[2], Fanny Richard[1], Sara Bonacchi[1], Dirk De Vos[4], Peter Lievens[3], Maarten Roeffaers[4], Johan Hofkens[2] and Paolo Samorì[1]

[1]ISIS & icFRC, Université de Strasbourg & CNRS, 8, allée Gaspard Monge, 67000 Strasbourg, France.
[2]Department of Chemistry, KU Leuven, Celestijnenlaan 200F, B-3001 Leuven, Belgium.
[3]Laboratory of Solid State Physics and Magnetism, KU Leuven, Celestijnenlaan 200D, B-3001 Leuven, Belgium.
[4]Department of Microbial and Molecular Systems, KU Leuven, Celestijnenlaan 200F, B-3001 Leuven, Belgium.

Small noble metal clusters can exhibit molecule-like behaviour in terms of their electronic transitions, and certain clusters of silver atoms have demonstrated pronounced catalytic and optical properties. However relatively little is known about the relationship between the electronic and structural properties of these metal structures and the way to control their nuclearity and location when they are grown in zeolite matrices. In this work we have systematically studied the role of framework topology, degree of silver exchange, negative framework charge, and the cationic species in the parent zeolite on the structural and luminescent properties of Ag clusters formed inside LTA and FAU zeolites. With control over these four key parameters we correlate the optical properties with the ionization potentials of the silver clusters, and ultimately tune the emission from the green to deep red, demonstrating photoluminescence quantum yields (PLQYs) of close to 100% in low silver loaded FAUY [Ag0.5].
In order to understand more about the origin of these exceptional PLQYs in FAU zeolites, we characterized the clusters using EXAFS. Fig. 1 shows the EXAFS and Fourier transform best fits of heat-treated FAUX [Ag1] measured at LISA-BM08 beamline at the ESRF.

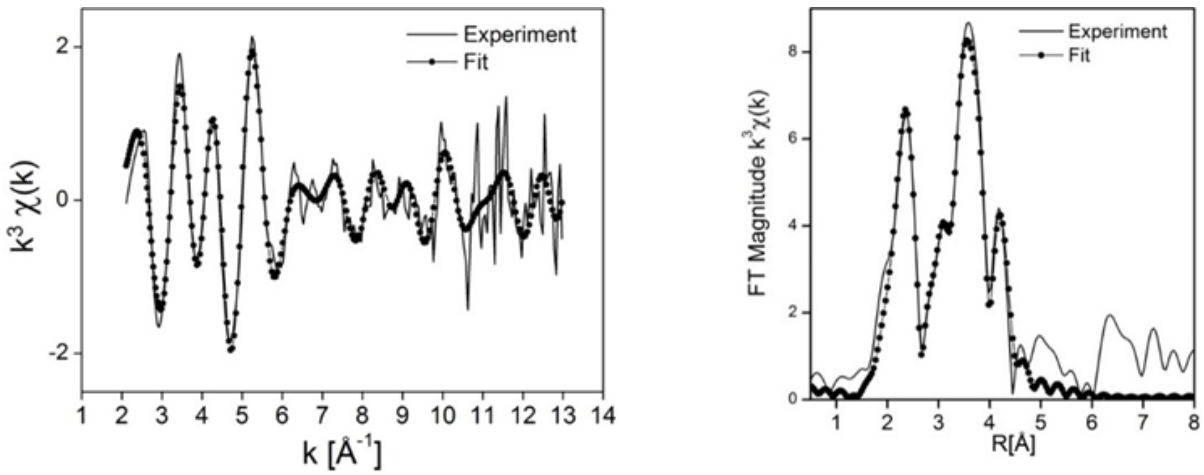

Figure 1. Transmission detected Ag K-edge k3-weighted EXAFS (a) with the corresponding phase corrected FT (b) best fits of heat-treated FAUX[Ag1] zeolite material

The first peak in the Fourier Transform (Fig. 1b) corresponds to multiple oxygen contributions reflecting he coordination of silver atoms with framework oxygen atoms and extra-framework water molecules. The second peak is mostly composed of two Ag-Si/Al contributions of Ag_R in the rings and Ag_P in the prisms of the zeolite framework plus an Ag-Ag contribution that corresponds to the remaining silver atoms (Ag_C) forming clusters inside the sodalite cage. It emerges from our data that, in the most luminescent material FAUY[Ag0.5], about 67% of silver atoms (Ag_C) form Ag_4 clusters inside the sodalite cages in which each Ag atom is bonded to 2.2 water molecules with the remaining about 33% of silver atoms being non-cluster-forming Ag_R and Ag_P cations. Similar EXAFS analysis of the less luminescent fully Ag-exchanged sample FAUY[Ag6.5] also reveals Ag_4 cluster structure, but with slightly fewer silver atoms involved in cluster formation. On the other hand, a significantly larger DebyeWaller factor associated with Ag_C-Ag_C shell is observed in FAUY[Ag6.5] than in FAUY[Ag0.5] indicating that Ag_4 clusters are significantly more ordered in FAUY[Ag0.5] than in fully loaded FAUY[Ag6.5]. These observations strongly suggest that the increase in quantum efficiency of Ag-FAUY zeolites with decreasing silver loading is driven by increasing order within the clusters rather than by changes in their nuclearity.

A totally different trend in PLQY is observed for FAUX with low Ag loaded FAUX[Ag1] featuring the lowest PLQY. EXAFS analysis shows that although Ag clusters have a nuclearity of about 4 in all our FAUX zeolites, a significantly lower proportion of silver atoms form clusters at low silver loadings than at high loadings consistent with the drop-off in PLQY at low silver loadings observed in FAUX. Closer analysis of the EXAFS signal of FAUX[Ag1] (Fig. 1) reveals a sodium shell around the silver clusters that could not be detected in FAUY. This strongly suggests that sodium ions, which are more concentrated and more mobile in FAUX compared with FAUY, are interfering with silver cluster formation. This highlights the important role played by counter-ions in luminescent cluster formation.

This EXAFS investigation shows that the high quantum efficiencies of our best materials that exceed all previous reports on luminescent silver clusters originate from an improved degree of order within Ag4 clusters located in the sodalite cages of the FAUY zeolite.

Publication: Fenwick, O et al., Nature Materials 2016, 15 (9), 1017-1022. DOI: 10.1038/NMAT4652

Size control of Pt Clusters on CeO2 Nanoparticles via an Incorporation-Segregation Mechanism and Study of Segregation Kinetics

F. Pilger[1,2], A. Testino[1], A. Carino[1,2], C. Proff[1,3], A. Kambolis[1,4], A. Cervellino[3], C. Ludwig[1,2]

[1]Paul Scherrer Institut (PSI), Energy and Environment Research Division,
[2]École Polytechnique Fédérale de Lausanne (EPFL), ENAC,
[3]PSI, Synchrotron Radiation and Nanotechnology Research Division, 4EPFL, EDCH

Noble metals supported on oxygen-deficient metal oxide materials represent ideal synergistic catalysts for several chemical processes, such as CO oxidation, since they are able to provide chemisorption centers for both CO (on highly dispersed noble metals, here Pt) and O_2 (on surface oxygen vacancies of the metal oxide, here CeO_2).[1] The contact points between the noble metal and metal oxide are often considered as the active catalytic centers. In order to increase the number of these catalytic centres the noble metal should be dispersed on the metal oxide surface in as small as possible entities. Hence, catalytic activity can be enhanced hy a higher surface area stemming from less material. Traditionally, catalysts are prepared by impregnation or deposition-precipitation methods followed by an appropriate thermal treatment to reduce the metal salts to metal particles. Recently, we presented a new wet synthesis method that allowed the preparation of Pt-doped CeO_2 (Pt:CeO_2) particles, with an average size smaller than 5 nm, using a one-pot procedure.[2,3] The ionically dispersed Pt segregates as subnanometric metallic Pt entities upon thermal treatment. Thus, starting from a single parent phase and by tuning the thermal treatment, it is possible to selectively achieve several scenarios along a continuum: from ionically dispersed noble metal incorporated into the host lattice (Pt:CeO_2), to partially segregated subnanometric Pt-clusters, to completely segregated Pt nanoparticles (Pt/CeO_2, Fig. 1).

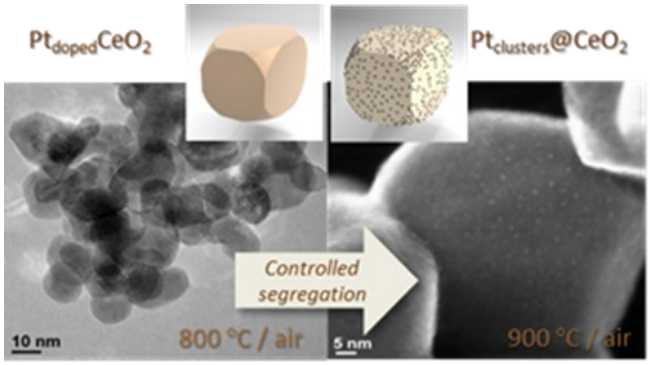

Figure 1:
From Pt:CeO_2 to Pt/CeO_2. The TEM and SE-STEM micrographs show the segregation of subnanometric Pt entities upon thermal treatment of ionically dispersed Pt on CeO_2. The process and its kinetics can be partly investigated by means of HR-XRD.

The Pt metal segregation kinetics were studied by ex-situ High Resolution X-Ray Diffraction (HR□XRD, Fig 2.1-2) at the MS beamline at the Swiss Light Source (SLS) and by X□ray Absorption Spectroscopy (XAS, Fig 2.3) at the LISA beamline at the ESRF Grenoble. With the latter we were able to determine that Pt is indeed ionically dispersed and to monitor the change of oxidation states for both Ce- and Pt-species (from the XANES region) and the respective change of coordination (from the EXAFS region). By means of several complementary techniques, such as (Scanning) Transmission Electron Microscopy ((S)TEM), Energy Dispersive X-Ray Spectroscopy (EDX) and catalytic testing, we were able to study the material and its behavior upon thermal treatment. We demonstrate that an unprecedented control over size of the metallic Pt0 clusters is achieved with this incorporation-segregation mechanism.

The obtained data helps to understand the nature of the active species for a specific reaction, to optimize the material functionalities, and to minimize the amount of noble metal required.[4-6] We further perform a kinetic study by in-situ HR-XRD measurements with the aim to estimate the activation energy for Pt clusters segregation and coalescence in air, which was found to be about 3.88 eV. This high activation energy indicates that Pt clusters are strongly anchored on the CeO2 surface and that their mobility is activated only at T>900 C. On the basis of thorough characterization, we present a possible segregation pathway under oxidizing conditions as opposed to a mere surface reduction during a reducing treatment, leading to the coalescence of less anchored Pt. This novel approach allows the preparation of catalysts with superior activity.[7]

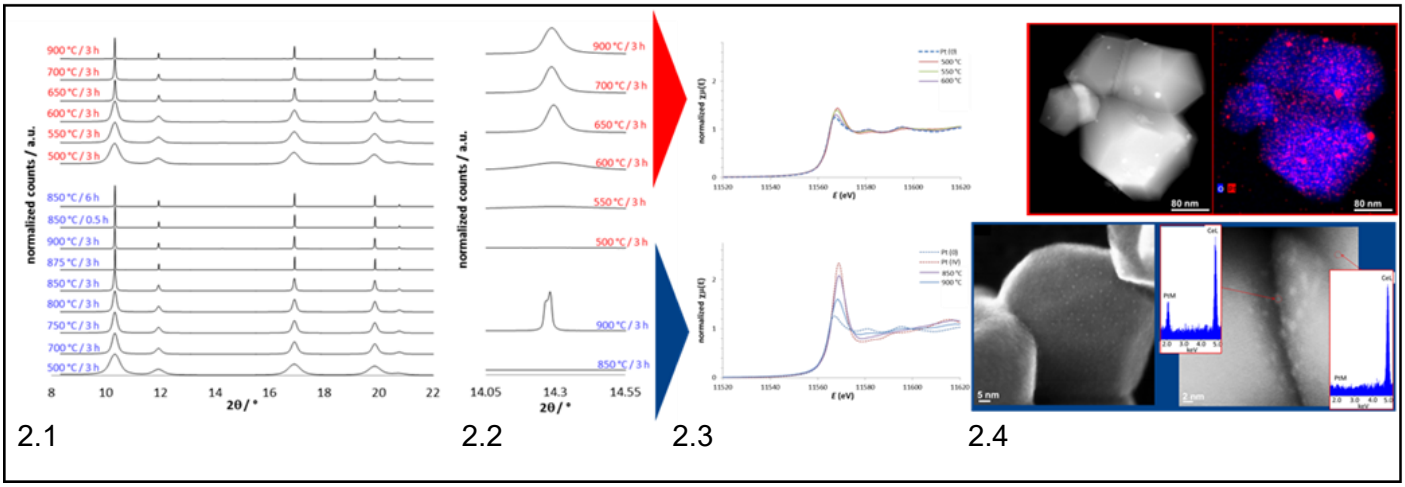

Figure 2.1: Ex-situ HRXRD characterization of various samples treated at different temperatures and/or durations in reducing (red) or oxidizing (blue) conditions. Figure 2.2: The evolution of previously absent Pt-peaks can be followed in blow-ups of the respective patterns. Figure 2.3: The corresponding XAS-data confirm the presence of Pt0 only in the samples treated above a certain segregation temperature. The Pt species have a mainly ionic character when treated at 850 °C in oxidizing conditions, whereas at 900 °C the spectrum shows mainly similarity with a metallic Pt reference. Under reducing conditions, the Pt species are already reduced at much lower temperatures, such as 500 °C. Figure 2.4: Further proof was found in STEM images and EDX signals.

Publication: F. Pilger et al. ACS Catal. 6 (2016), 3688. DOI: 10.1021/acscatal.6b00934

References:

1. M. Cargnello et al. Science 341 (2013), 771.

2. F. Pilger et al. J. Nanosci. Nanotechnol. 15(5) (2015), 3530.

3. A. Testino et al. Molecules 20 (2015) 10566.

4. F. Pilger et al. ACS Catal. 6 (2016), 3688.

5. A. Bruix et al. Angew. Chem. Int. Ed. 53 (2014), 10525.

6. S. K. Meher et al. Appl. Catal. B. 130-131 (2013), 121-131.

7. P. Bera et al. RSC Adv. 5 (2015), 94949.

Spectroscopic and electrochemical investigation of an efficient CuxO photocathode for H_2 evolution

T. Baran[1], S. Wojtyła[2], C. Lenardi[1], A. Vertova[1,3], P. Ghigna[3,4], E. Achilli[4], M. Fracchia[4], S. Rondinini[1,3], A. Minguzzi[1,3]

[1]University of Milan, [2]SajTom Light Future; [3]Consorzio INSTM – Firenze; [4]University of Pavia

Photoelectrocatalytic water splitting is one of the most promising approaches of light to chemical energy conversion, crucial for more sustainable development. In this report, a highly efficient copper(II) oxide photocathode is presented. The material, named Cu_xO-E is prepared from CuI nanoparticles and is initially partially reduced upon working conditions and soon reaches a stable form in which it can produce hydrogen for hours.
Calcination of nanocrystalline copper iodide directly on FTO glass (air atmosphere, T = 400°C) leads to a brown, mechanically stable electrode composed of CuO, with band gap energy 1.31 eV (from Diffuse Reflectance Spectroscopy) and flat band potential equal to 0.97 V vs. the reversible hydrogen electrode, RHE (from electrochemical impedance spectroscopy). Irradiation of the photoelectrode leads to a presence of cathodic photocurrent in a broad range of potential; the photocurrent increases with decreasing applied potential reaching the value of –1.2 mA cm□2 at 0.1 V vs RHE under solar simulator irradiation. The Incident Photon to Current Efficiency (IPCE) of under solar simulated light exceeds 22% for incident wavelength lower than 450 nm. The photocurrent densities depend on the electrolyte pH, reaching significantly higher values in alkaline and neutral pHs, while it shows lower values in acidic electrolyte. The efficiency of light conversion decreases significantly at the beginning of its work and then the material reaches a nearly stationary condition, since the photocurrent density does not change significantly with time up to more than 5 h. These results are confirmed by X-ray Photoelectron Spectroscopy: the photocathodes surface show an evident reduction upon irradiation in photoelectrochemical conditions, from a pure CuO to a Cu_2O-like state in case of electrode irradiated for 1 h. Even if a certain amount of CuO is present on the surface after 30 s, it is almost vanished after 1 h.

More detailed studies on the material have been performed using X-ray absorption spectroscopies at the LISA beamline, ESRF. XANES spectra (fig 1 A) shows that a freshly prepared electrode is composed only of copper(II) oxide while after its activity under photocathodic conditions the composition of the sample changes: CuO is partially reduced to Cu_2O (the weights of the linear combination being 0.8 - Cu_2O and 0.2 - CuO).

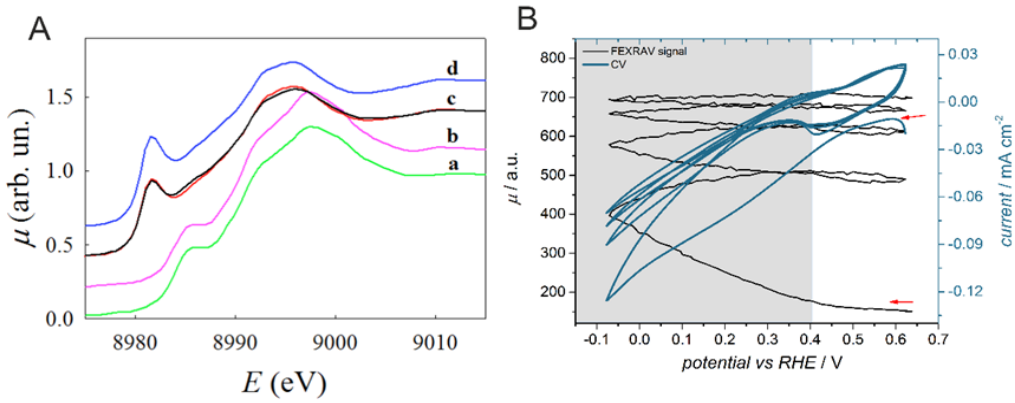

Figure 1 A: Cu-K edge XANES spectra of CuxO-E (b) and CuxO-E kept at 0.3 V vs RHE for 8 h upon irradiation with l = 400 nm (c, red line). The spectra of CuO (a) and Cu_2O (d) are shown for comparison. B: FEXRAV of CuxO at 8981 eV under LED illumination. Shadow zones indicate the instability potentials. Black curves: absorption coefficient; blue curves: current density. Starting points are indicated by red arrows. Both figures are adapte) with permission from ACS Appl. Mater. Interfaces 8 (2016), 21250−21260. Copyright 2016 American Chemical Society.

Moreover, fixed energy x-ray absorption voltammetry (FEXRAV) [1] is performed at 8981 eV (Cu-K edge), an energy value at which the maximum contrast between the absorption coefficient, μ, of Cu_2O and CuO is observed. In this technique, the electrode potential is swept and any variation of μ indicates a change of the oxidation state of the material. Experiments in dark and under irradiation indicates the increase of μ, and thus the reduction of material. The onset of the reduction potential is at about 0.25 V vs RHE in dark but under light it is shifted to less positive potentials (at about 0.4 V) as shown in fig 1 B. However, the increase in the FEXRAV signal decreases from cycle to cycle, indicating that the amount of Cu_2O formed in a single cycle decreases with time.

In conclusion, Cu_xO-E is an attractive photocathode for H2 evolution, due to its facile thermal preparation, high activity and good stability for hours.

Publication:
T. Baran et al., ACS Appl. Mater. Interfaces 8 (2016), 21250−21260. DOI: 10.1021/acsami.6b03345

[1] Minguzzi, A.; Lugaresi, O.; Locatelli, C.; Rondinini, S.; D'Acapito, F.; Achilli, E.; Ghigna, P. Fixed Energy X-Ray Absorption Voltammetry. Anal. Chem. 2013, 85, 7009−7013.

Aliovalent Doping in Colloidal Quantum Dots

A. Stavrinadis[1], J. S. Pelli Cresi[2], F. d'Acapito[3], C. Magén[4], F. Boscherini[2,3], and G. Konstantatos[1,5]

[1]ICFO-Institut de Ciencies Fotoniques, The Barcelona Institute of Science and Technology, 08860 Castelldefels (Barcelona), Spain
[2]Department of Physics and Astronomy, University of Bologna, Bologna, Italy
[3]Istituto Officina dei Materiali, Consiglio Nazionale delle Ricerche, c/o ESRF, Grenoble, France
[4]Laboratorio de Microscopías Avanzadas (LMA), Instituto de Nanociencia de Aragon (INA)-ARAID and Departamento de Fisica de la Materia Condensada, Universidad de Zaragoza, 50018 Zaragoza, Spain
[5]ICREA - Institució Catalana de Recerca i Estudis Avançats, Passeig Lluís Companys 23, 08010 Barcelona, Spain

Colloidal quantum dots (CQDs) are a class of nanomaterials whose unique optical properties has created a revolution in solution-processed photovoltaics, light-emitting diodes, and photodetectors. These applications require photoactive semiconductor components with accurately controlled optical and electronic properties. The lack of control over the electronic properties of CQD, in particular their doping character, still acts as a roadblock toward more-advanced device architectures and functionalities. Doping CQDs with aliovalent elements that can act as electron donors or acceptors is a very promising approach. Although aliovalent doping has been the cornerstone in doping single crystalline semiconductors to control carrier type and density, very few prior works report electronic doping with aliovalent cations for CQD solids and a complete understanding of the mechanisms at play has yet to be developed. Several semiconducting CQDs (CdSe, InAs, PbS) have been doped with a range of elements either during the synthesis, post-synthetically in solution, or via solid-state surface treatments. Yet, a complete picture of the factors that determine the efficacy and mechanism of dopant incorporation in the host, of the actual incorporation site of the dopant as well as the corresponding optoelectronic effects that doping causes, still remain elusive.

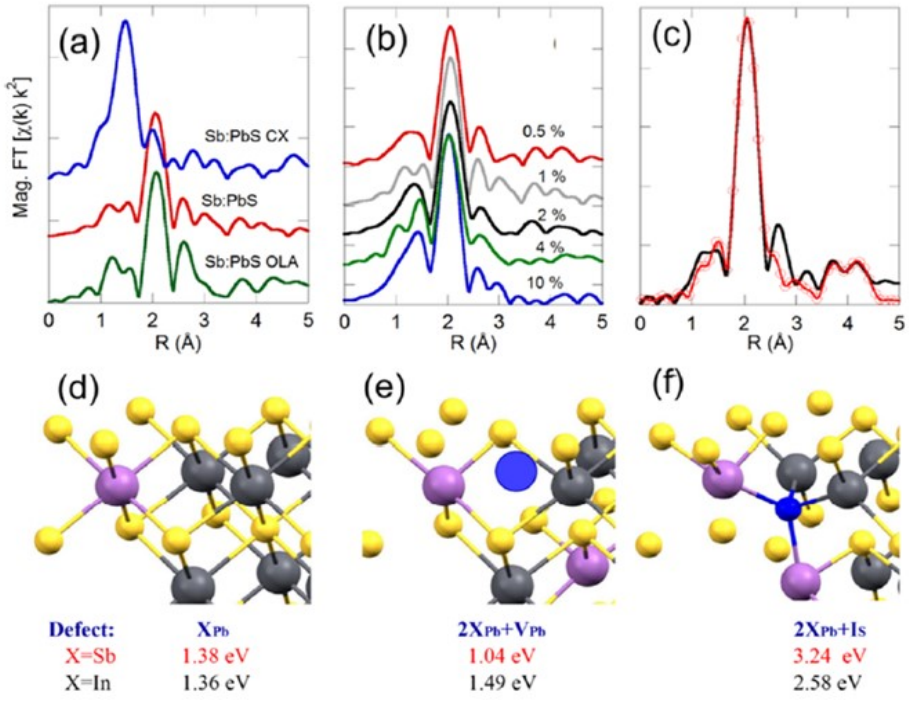

Figure x.1: Incorporation of dopants in the CQDs. Sb:PbS: Sb dopant incorporated during growth using a metal acetate; Sb:PbS CX: doping via a cation exchange process; Sb:PbS OLA: oleylamine added during growth to regulate the CQD growth process. (a−c) Magnitude of the Fourier transforms of Sb K-edge XAFS for 1% doped PbS CQD samples (panel (a)), for Sb:PbS samples, various compositions (panel (b)), and data (black continuous line) and fit (red line with markers) for 0.5% Sb:PbS sample (panel (c)). (d−f) Graphical representations and calculated formation energies for In and Sb dopants of the local atomic structure of the three dopant complexes considered: substitutional (panel (d)); double substitutional plus Pb vacancy (panel (e)); and double substitutional plus S interstitial (panel (f)). [Legend: yellow, matrix S; dark gray, matrix Pb; purple, dopant (Sb or In); dark blue, S interstitial; light blue, Pb vacancy.]

In this experiment we used XAFS to probe the local environment of PbS CQD doped with Sb and In. We studied various doping methods based on in – situ and post – synthetic dopant incorporation, described in the Figure caption. XAFS was used in a preliminary qualitative fashion to determine whether the dopant is actually incorporated in the PbS matrix or is predominantly found in an oxide phase on the surface of the CQD. From inspection of the XANES and EXAFS spectra we found that In is always found on the surface as an oxide phase; a similar situation was found in the Sb doped samples obtained by cation exchange, see panel (a) of the Figure. In the other Sb doped samples a significant incorporation of the dopant in the matrix was found.
Using a detailed analysis of the EXAFS spectra combined with ab – initio DFT simulations of candidate dopant incorporation sites we were able to propose that Sb is found predominantly in a neutrally charged complex formed by 2 Sb atoms substitutional to Pb atoms and a Pb vacancy, illustrated in panel (e); the corresponding best fit is reported in panel (c).

Publication:
A. Stavrinadis et al. , Chem. Mater. 2016, 28, 5384−5393. DOI: 10.1021/acs.chemmater.6b01445

A Pd/C-CeO_2 Anode Catalyst for High-Performance Platinum-Free Anion Exchange Membrane Fuel Cells

Hamish A. Miller[1], Alessandro Lavacchi[1], Francesco Vizza[1], Marcello Marelli[2], Francesco Di Benedetto[3], Francesco D'Acapito[4], Yair Paska[5], Miles Page[5] and Dario R. Dekel[6]

[1]CNR-ICCOM, Firenze, Italy, [2]CNR-ISTM, Milan, Italy, [3]Department of Earth Sciences, Università di Firenze, Firenze, Italy, [4]CNR-IOM-OGG c/o ESRF, Grenoble, [5]CellEra, Caesarea, Israel, [6]The Wolfson Department of Chemical Engineering, Technion, Israel Institute of Technology, Haifa, Israel

One of the biggest obstacles to the commercial exploitation of fuel cells is the cost. Most of this is due to the platinum (Pt) electrocatalyst that contributes for the 45% and more of the cost of whole systems. Complete removal of Pt from proton exchange membrane fuel cells (PEM-FCs) based on acidic electrolyte is a challenge of formidable difficulty. Anion exchange membrane fuel cells (AEM-FC) have been proposed as an alternative solution. Indeed, alkaline conditions allow the use of non-platinum electrocatalysts for both the Oxygen Reduction Reaction and the Hydrogen Oxidation Reaction (HOR). Nevertheless, the HOR, that is not an issue in conventional PEMFC, is sluggish in alkaline environment and the improvement of its rate is one of the major challenge for the AEM-FC technology. This is the reason why, despite the importance of the challenge, only a few examples of Pt-free AEM-FCs have been demonstrated till now. Here we report the results of our investigation on a novel Pt-free AEM-FC that employs a highly efficient mixed carbon-CeO_2 supported palladium (Pd) anode catalyst that has allowed a giant leap in the quest for novel material for the alkaline HOR. Our AEM-FC has delivered power densities exceeding 500 mW cm^2 in tests run on dry H_2. This value sets a new standard for AEM-FC that has only been possible thanks to the promotion of the HOR that has been achieved by the addition of CeO_2 to Pd.

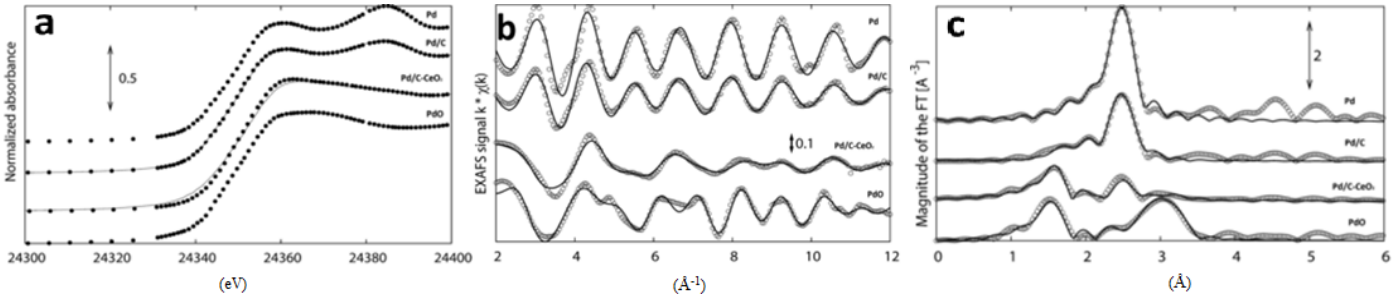

Figure.1: a) XAS at the Pd Kα edge of Pd/C-CeO_2 and Pd/C (XANES spectra of Pd-foil and PdO standards are also shown), b) EXAFS data and the related c) Fourier-transforms at the Pd Kα edge (transformation range 2.8–13.5 Å−1, k^2 weight). Dots are experimental data while continuous lines are calculated best-fit data.

To achieve the best promotion, effect a strong interaction between Pd and CeO_2 must occurs. Strong Pd-CeO_2 interactions would have a significant effect on the oxidation state of the Pd due to the oxide spillover capacity of ceria that would leave most of the Pd in the oxidized form. To verify this, we investigated the Pd oxidation state in the Pd/C and Pd/C-CeO_2 by X-ray absorption spectroscopy (XAS), comparing data with PdO and Pd standards. Figure 1a reports the comparison of the XANES region (X-ray absorption near edge structure), clearly showing that Pd in Pd/C-CeO_2 is mostly oxidized, while in Pd/C, palladium is prevalently in its metallic state. We also performed an EXAFS (extended X-ray absorption fine structure) analysis that was carried out modelling the data assuming a two component system consisting of metallic Pd and PdO. Figure 1b and 1c report the EXAFS and the related Fourier-transforms. Data analysis show that Pd (II) accounts for 87 wt. % of the total Pd content in Pd/C-CeO2. This is unusual as carbon supported Pd NPs (ca. 2nm in diameter) are usually at least 50% metallic, indeed, as expected, only 17 wt %of PdO was found in the Pd/C system.

The XAS investigation performed at the LISA beamline have therefore shown that for the Pd/C-CeO_2 catalysts Pd exists primarily as oxide also confirming that Pd is largely supported on the ceria regions. Such a structure not only leads to the weakening of the Pd-H bond, but also favours the fast transfer of OH- ions from ceria to Pd during catalysis. Both this aspect are responsible for the better performance in HOR of the Pd/C-CeO_2 catalyst in comparison with the Pd/C system.

Publication: H. A. Miller et al., Angew. Chem. Int. Ed. 55 (2016), 6004. DOI: 10.1002/anie.201600647

Dual Role of Zirconium Oxoclusters in Hybrid Nanoparticles: CrossLinkers and Catalytic Sites

Paolo Dolcet,[1,2,*] Cesare Benedetti,[3] Alessandro Cazzolaro,[1] Mauro Carraro,[1] Robert Graf,[3] Katharina Landfester,[3] Rafael Muñoz-Espí[3,4] and Silvia Gross[1,2,*]

[1]Dipartimento di Scienze Chimiche, Università degli Studi di Padova, Via Marzolo 1, 35131 Padova, Italy
[2]ICMATE-CNR, Via Marzolo 1, 35131 Padova, Italy
[3]Max Planck Institute for Polymer Research, Ackermannweg 10, 55128 Mainz, Germany
[4]Institut de Ciencia dels Materials (ICMUV), Universitat de Vale` ncia, C/Catedra` tic Jose´ Beltran 2, 46980 Paterna, Spain

Transition metal oxoclusters, with the general formula $M_xO_y(OH)_w(OC(O)R)_z$, are neutral complexes based on a polyhedral inorganic core, composed by M-O-M bridges (with M as transition metal typically in its highest oxidation state), coordinated by carboxylates (RC(O)O−) acting often as bidentate organic ligands. Zirconium-based oxoclusters have already been shown to be active for the homogeneous catalytic oxidation of sulfur-based substrates in the presence of hydrogen peroxide (F. Faccioli, et al., Eur. J. Inorg. Chem., 2015, 2015, 210–225). However, the oxoclusters showed low oxidative and hydrolytic stability under the explored conditions.
Owing to their tunable structure (in terms of composition, polyhedral arrangement, nuclearity, and functionalization), metal oxoclusters represent outstanding building blocks for the preparation of organic−inorganic hybrid materials. Particularly interesting are materials obtained by covalent incorporation of functionalized inorganic metal-based building blocks into a polymer matrix through copolymerization with suitable monomers (so-called class II organic−inorganic hybrid materials). Using this approach, a homogeneous distribution of inorganic components in the polymer matrix can be obtained, thus minimizing phase separation, aggregation, migration of the inorganic guest in the matrix, and leaching. The heterogenization of zirconium oxoclusters into a polymeric bulk matrix has been recently demonstrated to increase their overall stability, thus increasing their catalytic performances and enabling recovery and recycling (M. Vigolo et al., Appl. Catal. B Environ., 2016, 182, 636–644). After having tested the bulk materials, we recently demonstrated for the first time the successful radical copolymerization between the oxocluster $Zr_4O_2[O(O)CC(CH_3)=CH_2]_{12}$ (hereafter Zr_4) and methyl methacrylate in a direct (oil-in-water) miniemulsion system. We produced hybrid nanoparticles, containing functional Zr-based oxoclusters acting both as oxygen transfer catalysts as well as structural building blocks, with tunable behaviour in terms of dimensions, cross-linking degree, and swelling. The use of both anionic (sodium dodecyl sulfate SDS) and non-ionic (Lutensol AT50) surfactants for the stabilization of the miniemulsion was investigated.

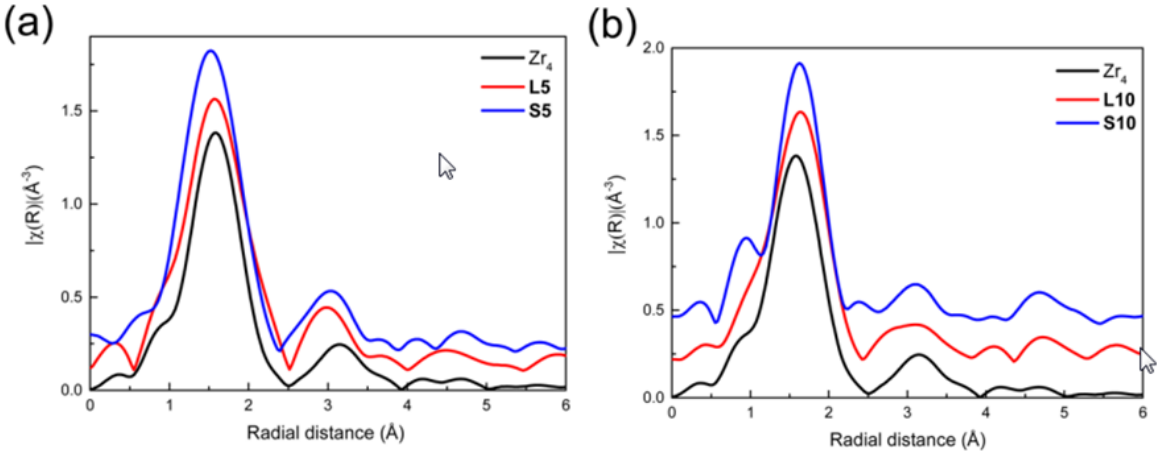

Figure 1: Fourier transforms of the Zr K-edge XAS spectra for the cross-linked hybrid poly(MMA-co-Zr4) nanoparticles compared to the Zr4 as a reference. The samples with (a) 5 wt % and (b) 10 wt % of Zr4 (synthesized using either SDS or Lutensol AT50 as surfactants) are shown.

X-ray absorption spectroscopy has been established as a versatile and unique tool for the evaluation of oxocluster stability upon embedding in hybrid materials (S. Gross and M. Bauer, Adv. Funct. Mater., 2010, 20, 4026–4047).

The structural integrity of the Zr4 oxocluster after the polymerization was investigated through X-ray absorption measurements at Zr K-edge, in fluorescence mode. The hybrid poly(MMA-co-Zr4) nanoparticles were analyzed and compared with the pristine Zr4 oxocluster. The difference between the reference Zr4 and L5 (5 wt % of oxocluster, Lutensol AT50 as surfactant) is minimal, which indicates that there is no relevant distortion in the oxocluster structure upon embedding. For sample S5 (5 wt % of oxocluster, SDS as surfactant), a small contraction in the first shell distance (corresponding to the Zr−O coordination polyhedra) and a broader peak are observed, indicating a distortion of the oxocluster structure. In contrast, samples prepared with higher amounts of oxocluster, the EXAFS curves indicate a distortion in the oxocluster for all samples, regardless of the surfactant used.

These minor distortion, on the other hand, do not seem to affect the catalytic activity of the embedded cluster for the two-step oxidation of methyl p-tolylsulfide (S) to the corresponding sulfoxide (SO) and sulfone (SO2) by hydrogen peroxide. As a general trend, the systems prepared with Lutensol AT50 are more efficient than the corresponding SDS-based systems, with initial TOF > 20, sulfide conversion >80% after 1 h, > 50% sulfone selectivity, with best results for L10, having TON = 1990, demonstrating a TON increase of 2 orders of magnitude with respect to the corresponding bulk polymer.

Publication: C. Benedetti et al., ACS Appl. Mater. Interfaces, 8 (2016), 26275−26284. DOI: 10.1021/acsami.6b07023

1. Achilli E., Minguzzi A., Visibile A., Locatelli C., Vertova A., Naldoni A., Rondinini S., Auricchio F., Marconi S., Fracchia M., Ghigna P. 3D-printed photo-spectroelectrochemical devices for in situ and in operando X-ray absorption spectroscopy Journal of Synchrotron Radiation 23 622-628 2016
2. Balerna A., Evangelisti C., Psaro R., Fusini G., Carpita A. Structural characterization of bimetallic Pd-Cu vapor derived catalysts Journal of Physics : Conference Series 712 012057-1-012057-4 2016
3. Baran T., Fracchia M., Vertova A., Achilli E., Naldoni A., Malara F., Rossi G., Rondinini S., Ghigna P., Minguzzi A., d'Acapito F. Operando and time-resolved X-ray absorption spectroscopy for the study of photoelectrode architectur Electrochimica Acta 207 16-21 2016
4. Baran T., Wojtyla S., Lenardi C., Vertova A., Ghigna P., Achilli E., Fracchia M., Rondinini S., Minguzzi A. An efficient CuxO photocathode for hydrogen production at neutral pH: New insights from combined spe ACS Applied Materials & Interfaces 8 21250-21260 2016
5. Benedetti C., Cazzolaro A., Carraro M., Graf R., Landfester K., Gross S., Muñoz-Espí R. Dual role of zirconium oxoclusters in hybrid nanoparticles: Cross-linkers and catalytic sites ACS Applied Materials & Interfaces 8 26275-26284 2016
6. Benzi F., Giuli G., Della Longa S., Paris E. VanadiumK-edge XANES in vanadium-bearing model compounds: A full multiple scattering study Journal of Synchrotron Radiation 23 947-952 2016
7. d'Acapito F., Pelli-Cresi S., Blanc W., Benabdesselam M., Mady F., Gredin P., Mortier M. The incorporation site of Er in nanosized CaF2 Journal of Physics: Condensed Matter 28 485301-1-485301-7 2016
8. d'Acapito F., Souchier E., Noé P., Blaise P., Bernard M., Jousseaume V. Chemical state of Ag in conducting bridge random access memory cells: A depth resolved X-ray absorpt Journal of Physics : Conference Series 712 012046-1-012046-4 2016
9. d'Acapito F., Souchier E., Noé P., Blaise P., Bernard M., Jousseaume V. Role of Sb dopant in Ag:GeSx-based conducting bridge random access memories Physica Status Solidi (a) 213 311-315 2016
10. d'Acapito F., Torrengo S., Xenogiannopoulou E., Tsipas P., Marquez Velasco J., Tsoutsou D., Dimoulas A. Evidence for Germanene growth on epitaxial hexagonal (h)-AlN on Ag(1 1 1) Journal of Physics Condensed Matter 28 045002-1-045002-8 2016
11. d'Acapito F., Trapananti A., Puri A. LISA: The italian CRG beamline for x-ray absorption spectroscopy at ESRF Journal of Physics : Conference Series 712 012021-1-012021-4 2016
12. Di Benedetto F., d'Acapito F., Bencistà I., Frizzera S., Caneschi A., Innocenti M., Lavacchi A., Montegrossi G., Oberhauser W., Romanelli M., Dittrich H., Pardi L.A., Tippelt G., Amthauer G. Geomaterials related to photovoltaics: A nanostructured Fe-bearing kuramite, Cu3SnS4 Physics and Chemistry of Minerals 43 535-544 2016
13. Fenwick O., Coutino-Gonzalez E., Grandjean D., Baekelant W., Richard F., Bonacchi S., De Vos D., Lievens P., Roeffaers M., Hofkens J., Samorì P. Tuning the energetics and tailoring the optical properties of silver clusters confined in zeolites Nature Materials 15 1017-1023 2016

14. Gibin G., Lorenzetti A., Callone E., Diré S., Dolcet P., Venzo A., Causin V., Marigo A., Modesti M., Gross S. Smart and covalently cross-linked: Hybrid shape memory materials reinforced through covalent bonds b ChemPlusChem 81 338-350 2016

15. Miller H.A., Lavacchi A., Vizza F., Marelli M., Di Benedetto F., d'Acapito F., Paska Y., Page M., Dekel D.R. A Pd/C-CeO2 anode catalyst for high-performance platinum-free anion exchange membrane fuel cells Angewandte Chemie International Edition 55 6004-6007 2016

16. Noé P., Sabbione C., Castellani N., Veux G., Navarro G., Sousa V., Hippert F., d'Acapito F. Structural change with the resistance drift phenomenon in amorphous GeTe phase change materials' thi Journal of Physics D 49 035305-1-035305-6 2016

17. Pethes I., Chahal R., Nazabal V., Prestipino C., Trapananti A., Michalik S., Jóvári P. Chemical short-range order in selenide and telluride glasses Journal of Physical Chemistry B 120 9204-9214 2016

18. Pilger F., Testino A., Carino A., Proff C., Kambolis A., Cervellino A., Ludwig C. Size control of Pt clusters on CeO2 nanoparticles via an incorporationsegregation mechanism and stu ACS Catalysis 6 3688-3699 2016

19. Rezvani S.J., Ciambezi M., Gunnella R., Minicucci M., Muñoz M.A., Nobili F., Pasqualini M., Passerini S., Schreiner C., Trapananti A., Witkowska A., Di Cicco A. Local structure and stability of SEI in graphite and ZFO electrodes probed by as K-edge absorption s Journal of Physical Chemistry C 120 4287-4295 2016

20. Rondinini S., Lugaresi O., Achilli E., Locatelli C., Minguzzi A., Vertova A., Ghigna P., Comninellis C. Fixed energy X-ray absorption voltammetry and extended X-ray absorption fine structure of Ag nanopar Journal of Electroanalytical Chemistry 766 71-77 2016

21. Rossi G., d'Acapito F., Amidani L., Boscherini F., Pedio M. Local environment of metal ions in phthalocyanines: K-edge X-ray absorption spectra Physical Chemistry - Chemical Physics 18 23686-23694 2016

22. Sanfilippo D. One-step hydrogen through water splitting with intrinsic CO2 capture in chemical looping Catalysis Today 272 58-68 2016

23. Sanson A. Displacive phase-transition of cuprite Ag2O revealed by extended x-ray absorption fine structure Journal of Physics and Chemistry of Solids 95 114-118 2016

24. Stavrinadis A., Pelli Cresi J.S., Magén C., Boscherini F., Konstantatos G. Aliovalent doping in colloidal quantum dots and its manifestation on their optical properties: Surfa Chemistry of Materials 28 5384-5393 2016

25. Tisato F., Marzano C., Peruzzo V., Tegoni M., Giorgetti M., Damjanovic M., Trapananti A., Bagno A., Santini C., Pellei M., Porchia M., Gandin V. Insights into the cytotoxic activity of the phosphane copper(I) complex [Cu(thp)4][PF6] Journal of Inorganic Biochemistry ee 2016

26. Urban S., Dolcet P., Möller M., Chen L., Klar P.J., Djerdj I., Gross S., Smarsly B.M., Over H. Synthesis and full characterization of the phase-pure pyrochlore Ce2Zr2O7 and the ¿-Ce2Zr2O8 phases Applied Catalysis B: Environmental 197 23-34 2016

27. Vachhani P.S., Sipr O., Bhatnagar A.K., Ramamoorthy R.K., Choudhary R.J., Phase D.M., Dalba G., Kuzmin A., Rocca F. Local structure and magnetization of ferromagnetic Cu-doped ZnO films: No magnetism at the dopant? Journal of Alloys and Compounds 678 304-311 2016

28. Zhang X., Lourenço-Martins H., Meuret S., Kociak M., Haas B., Rouvière J.L., Jouneau P.H., Bougerol C., Auzelle T., Jalabert D., Biquard X., Gayral B., Daudin B. InGaN nanowires with high InN molar fraction: Growth, structural and optical properties Nanotechnology 27 195704-1-195704-10 2016

Contacts

Beamline responsible:	Francesco d'Acapito dacapito@esrf.fr +33 4 7688 2426 , +33 6 8936 4302
Beamline scientists:	Alessandro Puri puri@esrf.fr +33 4 7688 2859
	Giovanni Lepore lepore@esrf.fr +33 4 7688 2530
Local Contact:	+33 6 8838 6994
Beamline:	+33 4 7688 2085
Laboratory:	+33 4 7688 2743
Skype:	gilda_beamline
Administration:	Fabrizio La Manna lamanna@esrf.fr +33 4 7688 2962
Web page:	http://www.esrf.eu/UsersAndScience/Experiments/CRG/BM08/

Forthcoming proposals submission deadlines

CRG quota: May, 8th, Nov. 8th 2017

ESRF quota: March 1st, Sept 10th 2017

Contributors to this issue

F. d'Acapito, A. Puri, G. Lepore (CNR-IOM, Grenoble)

A. de Luisa (CNR-IOM, Trieste)

E. Dettona (ESRF, Grenoble)

R. De Donatis (CNR, Genova)

F. Boscherini (Univ. Bologna)

D. Grandjean (KU Leuwen)

S. Gross, P. Dolcet (CNR-ICMATE and Univ. Padova)

A. Lavacchi (CNR-ICCOM, Firenze)

A. Minguzzi (Univ. Milano)

F. Pfilger (PSI, Viligen)